

## 层状钛硅酸盐化合物作为锂离子电池负极储能材料

刘美玼 胡宇翔 杜红宾\*

(南京大学化学化工学院, 配位化学国家重点实验室, 南京 210093)

**摘要:** 锂离子二次电池是手提设备的重要电力来源。近年来, 人们为了寻找更新颖更好的锂离子电极材料, 开始研究晶形离子交换材料, 这种材料具有开放孔道, 能够让离子在多孔框架里自由的进出。一种具有层状结构的钛硅酸盐 Na-JDF-L1 ( $\text{Na}_4\text{Ti}_2\text{Si}_8\text{O}_{22}\cdot 4\text{H}_2\text{O}$ ) 经过离子交换后被用作锂离子负极材料。它在循环 200 次后放电容量保持在  $364\text{ mAh}\cdot\text{g}^{-1}$ , 并且库伦效率约为 100%。通过将  $\text{TiO}_2$  引入 Li(Na)-JDF-L1 中, 有效的提高了材料的首次库伦效率和倍率放电性能。

**关键词:** 钛硅酸盐; 锂离子电池; 离子交换

中图分类号: TM912

文献标识码: A

文章编号: 1001-4861(2015)12-2425-07

DOI: 10.11862/CJIC.2015.315

## Layered Titanosilicates as Energy Storage Anode Materials for Lithium Ion Batteries

LIU Mei-Pin HU Yu-Xiang DU Hong-Bin\*

(State Key Laboratory of Coordination Chemistry, School of Chemistry and Chemical Engineering,  
Nanjing University, Nanjing 210093, China)

**Abstract:** Rechargeable lithium-ion batteries (LIBs) have become the dominant power source for portable devices. In search for new and better electrode materials for LIBs for future stationary storage, electronic devices and equipments, people have recently started to look over crystalline ion-exchange materials with open channels that facilitate fast lithium ion transportation through the porous network. Herein, the use of Li-exchanged titanosilicate Na-JDF-L1 with a layered structure as anode materials for LIBs was reported. It shows a discharge capacity of  $364\text{ mAh}\cdot\text{g}^{-1}$  after the 200th cycle with *ca.* 100% Coulombic efficiency and negligible loss of capacity, comparable with the lithium titanate anode. Furthermore, the incorporation of  $\text{TiO}_2$  in Li(Na)-JDF-L1 improves the electrochemical performance of the electrode with better initial Coulombic efficiency and higher rate performance.

**Key words:** titanosilicates; lithium ion batteries; ion-exchange

## 0 Introduction

Nowadays, rechargeable lithium-ion batteries (LIBs) have become the dominant power source for portable devices such as wireless phones, digital cameras and laptops, because of their superior energy density<sup>[1]</sup>. They are also the technology of choice for future hybrid electric vehicles, which could address

the reduction of  $\text{CO}_2$  emissions and air pollutions arising from transportation. To be used in electric vehicles or meet the further demands in portable devices, however, new rechargeable LIBs with much higher energy density, better recyclability and safety, and low cost are required. This calls for the developments of new high capacity and stable cathode and anode electrode materials for LIBs. In regard to

收稿日期: 2015-08-21。收修改稿日期: 2015-10-13。

国家重点基础研究发展计划(No.2011CB808704), 国家自然科学基金(No.21471075), 南京大学博士研究生提升计划 B 项目资助。

\*通讯联系人。E-mail: hbdu@nju.edu.cn

the anode materials for LIBs, many kinds of materials have been researched, such as alloy systems<sup>[2]</sup>, carbon or graphite<sup>[3]</sup>, titanate  $\text{Li}_4\text{Ti}_5\text{O}_{12}$  (LTO)<sup>[4]</sup> and so on. The carbon, graphite and carbon nanotubes have been put to use as the major commercial anode materials in LIBs, but it is not nearly enough to meet the requirement for future stationary storage, electric devices and equipment because of safety hazards<sup>[5]</sup> and high processing cost<sup>[5-7]</sup>. On the other hand, titanate-based materials have emerged as an attractive choice as anode materials. The three-dimensional spinel-structured LTO produce no volume change during the insertion and extraction of lithium ions<sup>[8]</sup>. However, the high operating voltage (1.5 V vs  $\text{Li}/\text{Li}^+$ ), the low capacity ( $175 \text{ mAh} \cdot \text{g}^{-1}$ ) and the poor electronic conductivity<sup>[9]</sup> are the shortcomings for LTO.

In search for better electrode materials for LIBs for future stationary storage, electric devices and equipment, people recently started to look over crystalline anionic frameworks with open channels that facilitate fast lithium ion transportation through the porous network<sup>[10]</sup>. Exemplary materials include  $\text{LiFePO}_4$ ,  $\text{LiMPO}_4\text{F}$  ( $\text{M}=\text{V}, \text{Fe}, \text{Ti}, \text{Mn}$ ),  $\text{LiFeSO}_4\text{F}$ ,  $\text{Li}_2\text{FeSiO}_4$ , *etc.*<sup>[11]</sup> which have been shown to be

promising cathode materials for LIBs. The use of anionic framework materials as an anode is rare, though the anionic framework titanate  $\text{Li}_4\text{Ti}_5\text{O}_{12}$  has been known as a promising candidate for anodic electrodes for LIBs<sup>[4,8-9]</sup>. As far back as 2002, Patoux and Masquelier<sup>[12]</sup> have investigated the lithium intercalation in  $\text{Li}_2\text{TiSiO}_4$ . Although there were no significant capacities in this nonporous titanasilicate phase, this study provided a new anode material from which to choose. Later, Luca and co-workers studied the lithium intercalation of a microporous titanasilicate known as sitinakite with the formula  $\text{Na}_2\text{Ti}_2\text{O}_3\text{SiO}_4 \cdot 2.76\text{H}_2\text{O}$ <sup>[13]</sup>, which consists of titania-like chains connected by  $\text{SiO}_4$  tetrahedra. The material showed some useful lithium intercalation capacity of *ca.*  $200 \text{ mAh} \cdot \text{g}^{-1}$  after 20th cycle, which compares favorably with those reported for rutile and  $\text{Li}_4\text{Ti}_5\text{O}_{12}$ . However, the material has poorer cycling properties and a smaller voltage plateau, which limit its application as a LIB anode material.

JDF-L1<sup>[14]</sup> (also called AM-1<sup>[15]</sup>) is a non-centrosymmetric layered titanasilicate of composition  $\text{Na}_4\text{Ti}_2\text{Si}_8\text{O}_{22} \cdot 4\text{H}_2\text{O}$ . It consists of anionic layers of small cages made up of eight  $\text{SiO}_4$  tetrahedra and one square-pyramidal  $\text{TiO}_5$  polyhedron (Fig.1a). The

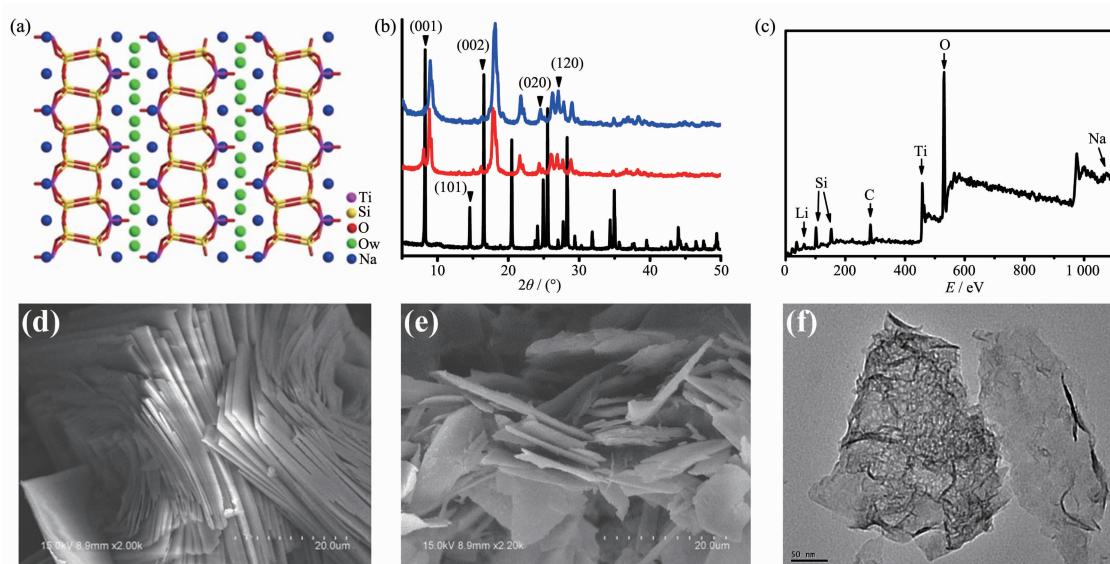


Fig.1 (a) View of the layered Na-JDF-L1 structure; (b) PXRD of as-synthesized (bottom), partly (middle) and fully (top)  $\text{Li}^+$ -exchanged JDF-L1; (c) XPS spectra of  $\text{Li}(\text{Na})$ -JDF-L1, Atomic Concentration of  $\text{Li}(\text{Na})$ -JDF-L1:  $\text{Li}1s$  4.74,  $\text{C}1s$  22.25,  $\text{O}1s$  51.29,  $\text{Na}1s$  1.59,  $\text{Si}2p$  11.29,  $\text{Ti}2p$  8.85; Atomic Concentration of As-prepared JDF-L1:  $\text{C}1s$  21.73,  $\text{O}1s$  48.33,  $\text{Na}1s$  10.56,  $\text{Si}2p$  11.74,  $\text{Ti}2p$  7.63; (d) SEM image of Na-JDF-L1; (e) SEM and (f) TEM images of  $\text{Li}(\text{Na})$ -JDF-L1

adjacent layers are separated by a layer of water molecules sandwiched between two layers of  $\text{Na}^+$  ions. The charge-balancing  $\text{Na}^+$  ions can be replaced by inorganic and organic pillars such as monoprotonated nonylamine<sup>[14,16]</sup>, which gives the possibility of lithium intercalation in LIBs. Therefore, we prepared the titanosilicate electrode by using Li-exchanged Na-JDF-L1 and tested its performance as an anode for LIBs. It showed much better discharge capacities with capacity retention than sitinakite, comparable to those of the LTO anode.

## 1 Experimental

### 1.1 Materials preparation

Na-JDF-L1 was made according to the modified literature<sup>[14]</sup>: 1.75 g of tetrabutyl orthotitanate (TBOT, 98%) and 6 mL of aqueous hydrogen peroxide (30%) were dropped into 12 mL of aqueous ammonia (25%) to give a clear yellow solution. 0.8 g of tetrabutylammonium bromide (TBABr), 0.55 g of sodium hydroxide and 1.2 g of fumed silica (99%) were then mixed with the above solution. After stirring for 3~4 h, the mixture with a molar ratio of  $n_{\text{SiO}_2}:n_{\text{TiO}_2}:n_{\text{Na}_2\text{O}}:n_{\text{TPABr}}:n_{\text{H}_2\text{O}_2}:n_{\text{NH}_3}:n_{\text{H}_2\text{O}}=1.0:0.25:0.48:0.12:2.5:8.0:36$  was heated in a Teflon-liner autoclave at 180 °C for 10 days. The products were recovered by filtration, washed with distilled water and dried at 80 °C. The  $\text{TiO}_2$ -Na-JDF-L1 was prepared by using the same procedure as above except that more TBOT ( $n_{\text{SiO}_2}:n_{\text{TiO}_2}=1:0.375$ ) were used. The  $\text{Li}^+$ -ion exchange reaction was carried out in a flask with 0.5 g of Na-JDF-L1 in 150 mL of 0.6 mol  $\cdot \text{L}^{-1}$   $\text{LiNO}_3$  solution, which was stirred in 100 °C for 24 h. The ion-exchange process was repeated for several times, and the products were recovered by filtration, washed with distilled water and dried at 80 °C.

### 1.2 Materials characterization

Powder X-ray diffraction (PXRD) patterns were collected in the  $2\theta=5^\circ\sim 50^\circ$  range with a scan speed of  $0.1^\circ \cdot \text{s}^{-1}$  on a Bruker D8 Advance instrument using a Cu  $K\alpha$  radiation ( $\lambda=0.15418\text{ nm}$ ) at RT. SEM images were obtained on a Hitachi S-4800 field-emission scanning electron microscope at an acceleration voltage of 5.0 kV. TEM images were obtained by

JEM-200CX transmission electron microscope. XPS spectra were obtained on a PHI 5000 Versaprobe.

### 1.3 Electrochemical measurements

The electrochemical performances of the materials were carried out in coin type cells. The as-synthesized active materials (Li-JDF-L1, Na-JDF-L1, Li(Na)-JDF-L1,  $\text{TiO}_2$ -Li(Na)-L1) were prepared as working electrodes (80%, *w/w*). They were well mixed with acetylene blacks (10%, *w/w*) and grounded in an agate mortar, and then blended into N-methyl pyrrolidinone (NMP) and Poly (vinylidene fluoride) (PVDF) (10%, *w/w*) at RT. The Cu foils as electrode current collectors were coated with the above slurries and dried at 120 °C in vacuum for 24 h. The electrode was then assembled into a coin-type (CR2032) cell with pure lithium foil (99.9%, Aldrich) as the counter electrode, polypropylene membrane (Celgard 2325) as the separator and 1 mol  $\cdot \text{L}^{-1}$   $\text{LiPF}_6$  in Ethylene carbonate (EC)/Dimethyl carbonate (DEC)/Ethyl Methyl Carbonate (EMC) (1:1:1, *V:V:V*) as the electrolyte in an argon-filled glove box (MBraun Co.). Cyclic voltammetry was carried out on a CHI660D electrochemical workstation at a  $0.2\text{ mV} \cdot \text{s}^{-1}$  scan rate. The charge and discharge cycles were tested galvanostatically on a bipolar system cell hardware (CT3008W, Neware battery testing system) with a voltage window between 0.01 and 3.0 V (vs  $\text{Li/Li}^+$ ) at RT.

## 2 Results and discussion

The obtained off-white solid Na-JDF-L1 was subject to lithium ion exchange. As shown in Fig.1b, PXRD studies showed that upon treatment, the intensities of the (001) peak of Na-JDF-L1 diminished significantly, and new peaks at higher angles appeared. The latter can be attributed to those of  $\text{Li}^+$ -exchanged JDF-L1, which has smaller interlayer spacings because of the smaller radii of  $\text{Li}^+$ . The interlamellar spacing corresponding to the (001) plane peak decreased from 1.07 nm in the as-synthesized Na-JDF-L1 to 0.92 nm in the  $\text{Li}^+$ -exchanged JDF-L1. X-ray photoelectron spectroscopy (XPS) measurements (Fig.1c) shows the existence of Li together with the residue of Na, indicating the incomplete ion-exchange

of  $\text{Na}^+$  (denoted as  $\text{Li}(\text{Na})\text{-JDF-L1}$ ). Further treatment can lead to complete replacement of  $\text{Na}^+$  by  $\text{Li}^+$  (denoted as  $\text{Li-JDF-L1}$ ), as shown by the disappearance of the (001) diffraction peak of  $\text{Na-JDF-L1}$ . The obtained  $\text{Li}(\text{Na})\text{-JDF-L1}$  and  $\text{Li-JDF-L1}$  samples shows weaker and broader diffraction peaks compared to the as-synthesized one, indicating that ion exchange led to an exfoliation and produced a wide distribution of the interlamellar spacings. There are several PXRD peaks at high angles, *e.g.*  $2\theta=24.14^\circ$  and  $27.04^\circ$ , remained unchanged at similar positions after ion exchange. They correspond to the crystallographic planes (020) and (120), respectively, and their positions are independent of the basal spacing. The presence of these peaks implies that the integrity of the titanosilicate layer is intact. The exfoliation is apparent from the SEM micrographs (Fig.1d~e), which show the flakes fallen off the large agglomerates of  $\text{Na-JDF-L1}$  crystals during ion exchange. TEM image (Fig.1f) shows wrinkle sheets with irregular intra-sheet distances as results of delamination.

The electrochemical performance of the ion-exchanged JDF-L1 was tested in the half cell in a CR2032 coin-type LIB. Fig.2a shows the first three cycles of the cyclic voltammetry (CV) profiles for partly ion-exchanged  $\text{Li}(\text{Na})\text{-JDF-L1}$  at a scan rate of  $0.2 \text{ mV} \cdot \text{s}^{-1}$  and a potential range of  $0.01 \sim 3.0 \text{ V}$ . There are three peaks at approximately 1.6, 1.1 and 0.5 V, respectively, in the cathodic scan of the first cycle. The anode branch from  $0.01 \sim 1.0 \text{ V}$  is smooth with a sharp slope, followed by an oxidation peak at *ca.* 1.1 V. In the subsequent 2nd and 3rd cycles, the cathode peaks at 1.6 and 0.5 V disappeared and the peak at 1.1 V shifted to *ca.* 0.9 V. In the meanwhile, the peak at 1.1 V in the anodic scan remained. These indicate that the former two peaks at 1.6 and 0.5 V correspond to non-reversible reactions, likely due to the reduction of  $\text{PF}_6$ -related species in the presence of moisture<sup>[17]</sup> and the formation of a solid electrolyte interphase (SEI) layer<sup>[18]</sup>, respectively. The peaks at  $1.1 \sim 0.9 \text{ V}$  in the cathodic scan of the first three cycles and the peaks centered at 1.1 V in the anodic scan can be related to the lithiation/delithiation of

JDF-L1, which is consistent with those observed in stinknite<sup>[13]</sup>.

Fig.2b shows the charge/discharge curves of the  $\text{Li}(\text{Na})\text{-JDF-L1}$  electrode cycled at a current density of  $100 \text{ mA} \cdot \text{g}^{-1}$ . The initial galvanostatic discharge curve drops sharply from 3.0 to 0.5 V and forms a plateau at  $0.15 \sim 0.12 \text{ V}$ . The first discharge capacity is  $1286 \text{ mAh} \cdot \text{g}^{-1}$  with a reversible charge capacity of  $254 \text{ mAh} \cdot \text{g}^{-1}$ . In the following discharge/charge process, the voltage curves display a similar profile and the electrochemical performance of  $\text{Li}(\text{Na})\text{-JDF-L1}$  electrode becomes stable. The discharge capacity for the

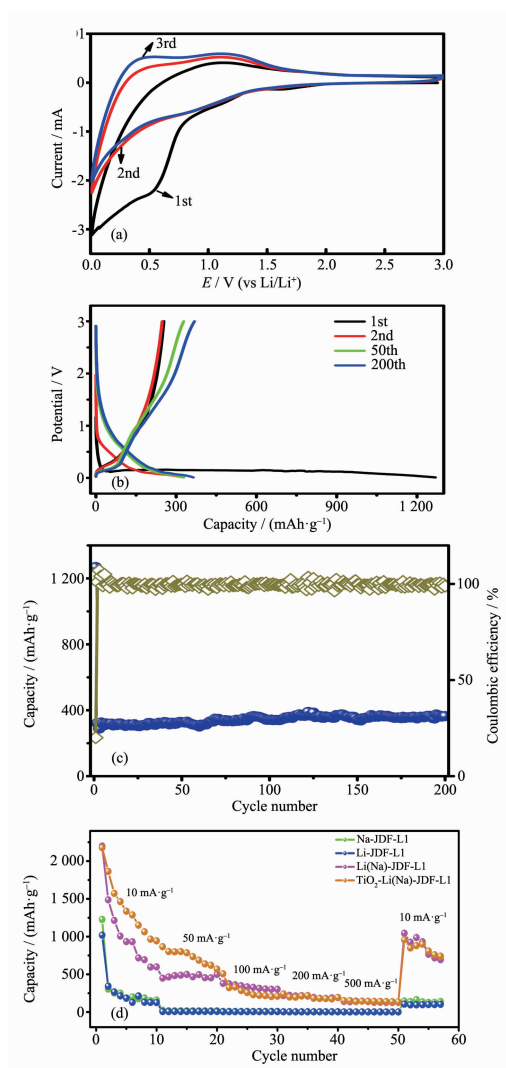


Fig.2 (a) First three CV profiles of  $\text{Li}(\text{Na})\text{-JDF-L1}$ ; (b) Charge-discharge curves of the  $\text{Li}(\text{Na})\text{-JDF-L1}$  electrode; (c) Capacity retention of the  $\text{Li}(\text{Na})\text{-JDF-L1}$  electrode; (d) Rate capacity of the JDF-L1 electrodes at various current densities



2nd, 50th and 200th cycles is 321, 317 and 368  $\text{mAh} \cdot \text{g}^{-1}$ , respectively. The irreversible capacity in the initial discharge/charge process may be attributed to the formation of solid electrolyte interface (SEI) film<sup>[19]</sup> on the surface of Li(Na)-JDF-L1, and irreversible reactions between the electrode and electrolyte, e.g. the generation of lithium salt and some of Li remained in the electrolyte<sup>[20]</sup>. This corroborates with the CV measurements.

Fig.2c shows the curves of capacity and Coulombic efficiency cycled at a current density of  $100 \text{ mA} \cdot \text{g}^{-1}$ . It shows that the Li(Na)-JDF-L1 electrode exhibited a good cycling performance. Despite Li(Na)-JDF-L1 showing a low Coulombic efficiency of  $\sim 20\%$  in the first discharge/charge process, it recovered to *ca.* 100% in the second cycle, and maintained almost 100% in the subsequent cycles. The low Coulombic efficiency may be attributed to the irreversible intercalation of Li ions and decomposition of the electrolyte to some extent; On the other hand, the electrochemical action of the small amount water in the framework channels would need more current on the initial discharge, also resulting in an irreversible reduction reactions and a higher initial capacity<sup>[13]</sup>. Furthermore, the Li(Na)-JDF-L1 electrode exhibited both a high discharge capacity and a high Coulombic efficiency even after 200 cycles. The discharge capacity of the electrode is  $364 \text{ mAh} \cdot \text{g}^{-1}$  at the 200th cycle with *ca.* 100% efficiency, which is better than the LTO anode<sup>[4,8-9]</sup>. It is noted that the capacities became higher from the 70th to 200th discharge/charge cycles in comparison with that of the 2nd cycle, which may be resulted from the influence of the SEI films<sup>[21]</sup>. The good cycling performance of Li(Na)-JDF-L1 anode may be attributed to the crystalline anionic layer structure of JDF-L1, which limits the possibility of volume change during the lithium insertion/extraction. *Ex situ* PXRD studies of the cycled Li(Na)-JDF-L1 electrodes show the remaining layer structure (Fig.3), supporting this thesis. The rate capacity of the Li(Na)-JDF-L1 electrode was evaluated in the potential range of 0.01 ~ 3.0 V with the cell each discharged/charged 10 times at a current density

of 10, 50, 100, 200, 500 and then  $10 \text{ mA} \cdot \text{g}^{-1}$ , respectively. As shown in Fig.2d, the average discharge capacity of the Li(Na)-JDF-L1 electrode is over  $600 \text{ mAh} \cdot \text{g}^{-1}$  at  $10 \text{ mA} \cdot \text{g}^{-1}$ , and decreased to *ca.* 449, 379, 217 and  $140 \text{ mAh} \cdot \text{g}^{-1}$  at a higher current density of 50, 100, 200, and  $500 \text{ mA} \cdot \text{g}^{-1}$ , respectively. It then recovered back to *ca.*  $765 \text{ mAh} \cdot \text{g}^{-1}$  at a rate of  $10 \text{ mA} \cdot \text{g}^{-1}$ . The results showed that Li (Na)-JDF-L1 displayed a stable cycling behaviour at different current densities. This rate capability is, however, inferior to that of the LTO anode<sup>[4,8-9]</sup>, which has much better rate capacity retention at high current densities. This could probably be attributed to the poor electronic conductivity of the titanasilicate framework.

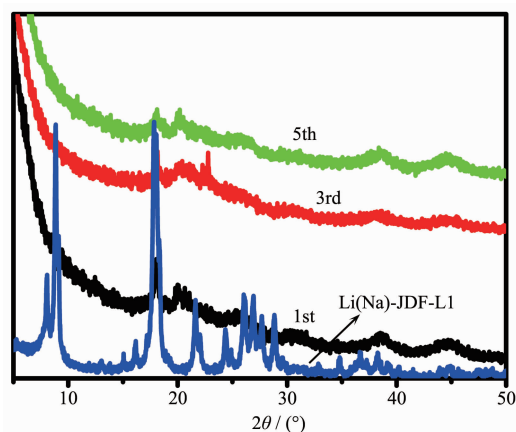


Fig.3 PXRD patterns of partly exchanged Li(Na)-JDF-L1, and the recovered Li(Na)-JDF-L1 electrodes after 1st, 3rd, and 5th cycles

To improve the rate performance of the Li(Na)-JDF-L1 electrode, the strategy of casting electronically conductive layers onto the surface of Li (Na)-JDF-L1 was attempted. Such a strategy has been demonstrated to be efficient for improving the rate capability of LTO by shortening the transport lengths of both lithium ions and electrons<sup>[8]</sup>. The addition of more tetrabutyl orthotitanate ( $n_{\text{SiO}_2} : n_{\text{TiO}_2} = 1 : 0.375$ ) into the synthesis mixture resulted in Na-JDF-L1 mixed with amorphous  $\text{TiO}_2$  (Fig.3~4). XPS spectra (Fig.4) show the peaks at 457.6( $\text{Ti}2p_{3/2}$ ) and 463.6 eV ( $\text{Ti}2p_{1/2}$ ) owing to  $\text{TiO}_2$ <sup>[22]</sup>. As shown in Fig.2d, the presence of  $\text{TiO}_2$  in Li(Na)-JDF-L1 resulted in an improved rate performance. The average capacities for  $\text{TiO}_2$ -Li(Na)-JDF-L1 are 270 and  $152 \text{ mAh} \cdot \text{g}^{-1}$  at 200 and  $500 \text{ mA} \cdot \text{g}^{-1}$ ,

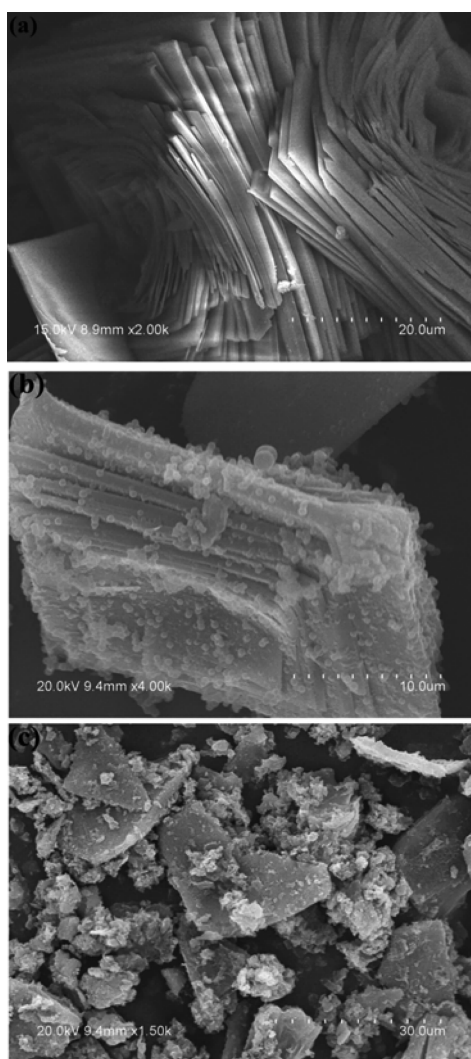


Fig.4 SEM images of Na-JDF-L1 (a), TiO<sub>2</sub>-Na-JDF-L1 (b) and TiO<sub>2</sub>-Li(Na)-JDF-L1 (c)

respectively, which are higher than those of the Li(Na)-JDF-L1 electrode without TiO<sub>2</sub> doping (*i.e.* 217 and 140 mAh·g<sup>-1</sup>, respectively).

Furthermore, the TiO<sub>2</sub>-Li(Na)-JDF-L1 electrode showed improved initial Coulombic efficiency of 85% (67% for the Li(Na)-JDF-L1 electrode at 10 mA·g<sup>-1</sup>). It is noted that both the pristine Na-JDF-L1 and fully exchanged Li-JDF-L1 showed poor electrochemical performance. The stable discharge capacities for pristine Na-JDF-L1 and fully exchanged Li-JDF-L1 are only *ca.* 140 and 100 mAh·g<sup>-1</sup> at 10 mA·g<sup>-1</sup>, respectively. Furthermore, both lost lithium intercalation ability at higher current densities. The poor electrochemical performance of the latter two materials may be due to the Na<sup>+</sup> or Li<sup>+</sup> occupying the

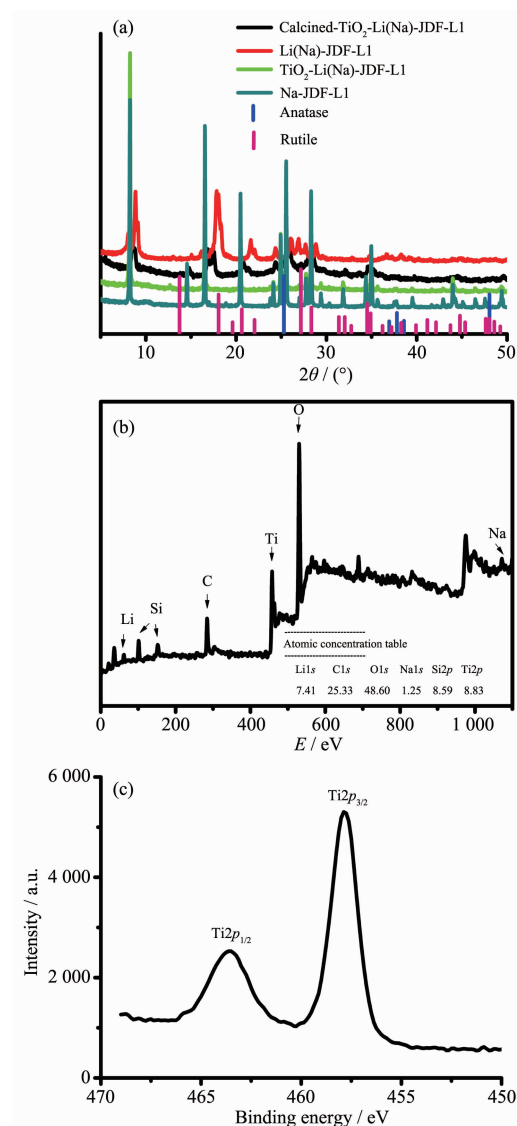


Fig.5 (a) PXRD patterns of TiO<sub>2</sub>-Na-JDF-L1 and TiO<sub>2</sub>-Li(Na)-JDF-L1, compared with those of Li(Na)-JDF-L1, anatase and rutile; (b) XPS spectra of TiO<sub>2</sub>-Li(Na)-JDF-L1; (c) High-resolution spectra of Ti(In TiO<sub>2</sub>,  $E(\text{Ti}2p_{3/2})=457.6$  eV,  $E(\text{Ti}2p_{1/2})=463.6$  eV)

sites in the framework which are designed for electrochemically inserted Li, similar to those observed in sitinakite<sup>[13]</sup>. The partial exchange of Na<sup>+</sup> by Li<sup>+</sup> likely opens up channels for Li<sup>+</sup> ion transportation between the cathode and the anode, leading to good electrochemical performance in Li(Na)-JDF-L1.

### 3 Conclusions

We prepared a titanosilicate anode for lithium ion battery by using a partly Li-exchanged Na-JDF-L1

with an anionic layered structure. The electrode showed a discharge capacity of  $364 \text{ mAh} \cdot \text{g}^{-1}$  after the 200th cycle with *ca.* 100% Coulombic efficiency and negligible loss of capacity, which is better than the LTO anode. It is postulated that the unique anionic layered structure can adapt to the volume expansion during cycling, leading to good recycle performance. Furthermore, the incorporation of  $\text{TiO}_2$  in  $\text{Li}(\text{Na})\text{-JDF-L1}$  improves the electrochemical performance of the electrode with better initial Coulombic efficiency and higher rate performance. The facile preparation, low cost, and the high reversible capacity with excellent recyclability of JDF-L1 suggest that titanosilicates with an anionic layered or framework structure may be a class of anode candidates for high-performance LIBs.

## References:

- [1] (a) Tarascon J M, Armand M. *Nature*, **2001**, **414**:359-367  
(b) Choi N S, Chen Z H, Freunberger S A, et al. *Angew. Chem. Int. Ed.*, **2012**, **51**:9994-10024
- [2] (a) Chan C K, Patel R N, O'Connell M J, et al. *ACS Nano*, **2010**, **4**:1443-1450  
(b) Hatchard T D, Dahn J R. *J. Electrochem. Soc.*, **2004**, **151**:A838-A842  
(c) Idota Y, Kubota T, Matsufuji A, et al. *Science*, **1997**, **276**:1395-1397  
(d) Park C M, Sohn H J. *Adv. Mater.*, **2007**, **19**:2465-2466
- [3] (a) Wu Y P, Holze R. *J. Solid State Electrochem.*, **2003**, **8**:73-78  
(b) Chang J C, Tzeng Y F, Chen J M, et al. *Electrochim. Acta*, **2009**, **54**:7066-7070
- [4] (a) Jung H G, Jang M W, Hassoun J, et al. *Nat. Commun.*, **2011**, **2**:516  
(b) Shen L F, Uchaker E, Zhang X G, et al. *Adv. Mater.*, **2012**, **24**:6502-6506
- [5] Fleischhammer M, Waldmann T, Bisle G, et al. *J. Power Sources*, **2015**, **274**:432-439
- [6] Fulvio P F, Brown S S, Adcock J, et al. *Chem. Mater.*, **2011**, **23**:4420-4427
- [7] (a) Schnorr J M, Swager T M. *Chem. Mater.*, **2011**, **23**:646-657  
(b) Goodenough J B, Kim Y. *Chem. Mater.*, **2010**, **22**:587-603  
(c) Manthiram A. *J. Phys. Chem. Lett.*, **2011**, **2**:176-178
- [8] (a) Prakash A S, Manikandan P, Ramesha K, et al. *Chem. Mater.*, **2010**, **22**:2857-2863  
(b) Wang Y Q, Gu L, Guo Y G, et al. *J. Am. Chem. Soc.*, **2012**, **134**:7874-7879  
(c) Li C C, Li Q H, Chen L B, et al. *ACS Appl. Mater. Interfaces*, **2012**, **4**:1233-1238
- [9] Amine K, Belharouak I, Chen Z, et al. *Adv. Mater.*, **2010**, **22**:3052-3057
- [10] (a) Koudriachova M V, Harrison N M, de Leeuw S W. *Solid State Ionics*, **2003**, **157**:35-38  
(b) Vu A, Qian Y, Stein A. *Adv. Energy Mater.*, **2012**, **2**:1056-1085
- [11] (a) Rangappa D, Murukanahally K D, Tomai T, et al. *Nano Lett.*, **2012**, **12**:1146-1151  
(b) Ellis B L, Makahnouk W R M, Makimura Y, et al. *Nat. Mater.*, **2007**, **6**:749-753  
(c) Recham N, Chotard J N, Dupont L, et al. *Nat. Mater.*, **2010**, **9**:68-74  
(d) Barpanda P, Ati M, Melot B C, et al. *Nat. Mater.*, **2011**, **10**:772-779  
(e) Tripathi R, Ramesh T N, Ellis B L, et al. *Angew. Chem. Int. Ed.*, **2010**, **49**:8738-8742
- [12] Patoux S, Masquelier C. *Chem. Mater.*, **2002**, **14**:5057-5068
- [13] Milne N A, Griffith C S, Hanna J V, et al. *Chem. Mater.*, **2006**, **18**:3192-3202
- [14] (a) Roberts M A, Sankar G, Thomas J M, et al. *Nature*, **1996**, **381**:401-403  
(b) Du H, Fang M, Chen J, et al. *J. Mater. Chem.*, **1996**, **6**:1827-1830
- [15] (a) Anderson M W, Terasaki O, Oshuna T, et al. *Philos. Mag. B*, **1995**, **71**:813-841  
(b) Lin Z, Rocha J, Brando P, et al. *J. Phys. Chem.*, **1997**, **101**:7114-7120
- [16] Rubio C, Casado C, Gorgojo P, et al. *Eur. J. Inorg. Chem.*, **2010**, **1**:159-163
- [17] Aurbach D, Zaban A. *J. Electroanal. Chem.*, **1995**, **393**:43-53
- [18] Cao Y, Xiao L, Ai X, et al. *Electrochem. Solid State*, **2003**, **6**:A30-A33
- [19] (a) Tang M, Newman J. *J. Electrochem. Soc.*, **2012**, **159**:A1922-A1927  
(b) Park M S, Kim J H, Jo Y N, et al. *J. Mater. Chem.*, **2011**, **21**:17960-17966
- [20] Yan N, Wang F, Zhong H, et al. *Sci. Rep.*, **2013**, **3**:1568
- [21] (a) Spotnitz R, Franklin J. *J. Power Sources*, **2003**, **113**:81-100  
(b) Lee S B, Pyun S I. *Carbon*, **2002**, **40**:2333-2339  
(c) He Y B, Liu M, Huang Z D, et al. *J. Power Sources*, **2013**, **239**:269-276
- [22] Jouan P Y, Peignon M C, Cardinaud C, et al. *Appl. Surf. Sci.*, **1993**, **68**:595-603